

*Letter to the Editor***A thin H I circumnuclear disk in NGC 4261****H.J. van Langevelde¹, Y.M. Pihlström², J.E. Conway², W. Jaffe³, and R.T. Schilizzi^{1,3}**¹ Joint Institute for VLBI in Europe, Postbus 2, 7900 AA, Dwingeloo, The Netherlands² Onsala Space Observatory, 439 92 Onsala, Sweden³ Sterrewacht Leiden, Postbus 9513, 2300 RA, The Netherlands

Received 30 November 1999 / Accepted 19 December 1999

Abstract. We report on high sensitivity, spectral line VLBI observations of the H I absorption feature in the radio galaxy NGC 4261. Although absorption is only detectable on the most sensitive baseline, it can be unambiguously associated with the counterjet and is interpreted to originate in a thin atomic circumnuclear disk. This structure is probably a continuation of the dusty accretion disk inferred from HST imaging, which could be feeding the massive black hole. H I column densities in front of the counterjet of the order of $10^{21} (T_{sp}/100 \text{ K}) \text{ cm}^{-2}$ are derived, consistent with X-ray data and VLBI scale free-free absorption. The data presented here are the result of the first scientific project processed on the new EVN MkIV data processor.

Key words: galaxies: active – galaxies: individual: NGC 4261 – radio lines: galaxies

1. Introduction

Perhaps the most striking feature of the FRI radio galaxy NGC 4261 (3C 270) is its approximately 240 pc radius circumnuclear dust disk revealed by HST observations (Jaffe et al. 1993). Further optical observations of the kinematics of emission lines in the inner regions of this disk by Ferrarese et al. (1996) have since provided evidence for a central black hole of mass of $4.9 \times 10^8 M_{\odot}$. In the radio band, H I absorption has been detected toward the core of NGC 4261 using the VLA (Jaffe & McNamara 1994). It was argued by these authors that this absorption is due to atomic hydrogen in the inner part of the HST disk. Such a disk interpretation is consistent with high resolution VLBI or MERLIN H I absorption observations in a number of other AGN. For example VLBA H I observations of another FRI galaxy, Hydra A, are consistent with a 20 pc flattened disk structure (Taylor 1996). In this Letter we report on VLBI observations of NGC 4261 performed using the high-sensitivity antennas of the European VLBI Network (EVN). The aims were to confirm that the H I is indeed associated with the

HST dust disk and to better constrain the disk geometry and physical properties.

Detailed studies of the dynamics and chemistry of circumnuclear disks such as that found in NGC 4261 are important for several reasons. Such disks almost certainly provide the fuel which powers AGN, but the accretion process is poorly understood. In addition such flattened circumnuclear structures are required by orientation-based unified schemes. While the inner edges of these occulting structures must be on BLR scales (0.1 – 1 pc) their outer radii are poorly defined and may extend to hundreds of parsecs. Evidence for circumnuclear gas on a variety of scales in different physical states has been accumulating. Examples include HST imaging of parsec scale ionised gas in M87 (Ford et al. 1994), 100 – 1000 pc scale molecular CO in Centaurus A (Rydbeck et al. 1993) and HCN in the Seyfert 2 NGC 1068 (Tacconi et al. 1994). Amongst all the objects observed NGC 4261 is unique in showing optical dust, H I absorption and VLBI scale free-free absorption (Jones & Wehrle 1997), allowing us to study the disk on a variety of scales.

The HST optical imaging of NGC 4261 provides strong constraints on the disk geometry at 100 pc scales. The ratio of the apparent major and minor axes (Ferrarese et al. 1996, Jaffe et al. 1996) implies, if the disk is circular, that its normal is inclined 64° to the line of sight. Modeling of the dust obscuration shows that it is the East side of the disk which is closest to us. Such modeling also shows that the dust disk is thin, with a thickness < 40 pc at its outer edge (Jaffe et al. 1996). The normal to the disk is found in projection to be roughly oriented along the radio axis, making an angle of 14° to the kiloparsec scale radio jets. At both 1.6 and 8.4 GHz VLBI observations show a two-sided jet in the same position angle as the kiloparsec jets (Jones & Wehrle 1997). The Eastern jet, which is slightly weaker, is assumed to be the counterjet, given that the Eastern edge of the HST dust disk is tilted toward us and the radio jets are roughly aligned along the disk axis. Consistent with this orientation, Jones & Wehrle (1997) argue that a narrow gap in the 8.4 GHz radio emission toward the Eastern jet is from free-free absorption via occultation by an inner ionised accretion disk of radius 0.2 pc. In the remainder of the paper we discuss our H I VLBI observations and the additional constraints on disk geometry

and physical properties they provide. Throughout this paper we assume a distance of ~ 30 Mpc (Nolthenius 1993), so 1 mas corresponds to 0.14 pc.

2. Observations and processing

Observations of NGC 4261 were made at 21 cm with the European VLBI Network (EVN) on February 22 1999 and lasted 10 hours. Participating antennas were Effelsberg, Jodrell Bank (Lovell telescope), Medicina, Noto, Onsala, Torun, and Westerbork (phased array). Unfortunately one of the three large collecting areas, the 100m at Effelsberg, was unable to observe due to heavy snowfall. The observing mode consisted of 4 frequency bands, all observed with dual circular polarisation, 4 MHz wide and 2-bit sampled. The second frequency band was centred on the H I line of NGC 4261 at a velocity of 2237 km/s (heliocentric, optical definition) corresponding to a frequency of 1410 MHz.

The data were processed on the EVN MkIV data processor at the Joint Institute for VLBI in Europe (JIVE) and constitute the first scientific experiment to be carried out with this new facility. The data were correlated between July 26 and August 6 1999 in two passes; the first resulting in 128 spectral channels on both polarisations of the line data, the second pass yielding sensitive continuum data, by processing all basebands with modest spectral resolution. For the spectral line dataset the resulting spectral resolution from uniform weighting was ≈ 7.4 km/s. Data quality was good, except for some bad tape passes from Torun and a large fraction of the data for Medicina which was corrupted by interference. Amplitude calibration was carried out in the standard way using the T_{sys} values and gain curves from the stations. The continuum was imaged using standard self-calibration and CLEAN deconvolution methods. From variations in amplitude gain factor in the final step of amplitude self-calibration we estimate the uncertainties in the overall flux density scales of our images to be of order 15%.

3. Results

The continuum image obtained of NGC 4261 is shown in Fig. 1. The noise level in this image is 0.35 mJy/beam. We find that the Western jet is somewhat brighter and more extended than the Eastern one, consistent with the VLBA maps of Jones & Wehrle (1997). From these VLBA maps it is clear that the flat spectrum core lies close to the peak of Fig. 1. We were able to fit a three component Gaussian model to the continuum visibility data, consisting of one compact core component and two jet components 18 and 14 mas (2.5 and 2 pc) to the East and West respectively.

In order to detect the weak H I absorption the spectral line data was self-calibrated with the continuum image, and then the continuum was subtracted using the AIPS task UVLIN. The spectral absorption was unambiguously detected on the Jodrell Bank – Westerbork baseline (Fig. 2). Other baselines did not have sufficient sensitivity to give any detections. From the phase information (not shown) it is clear that the absorption is not cen-

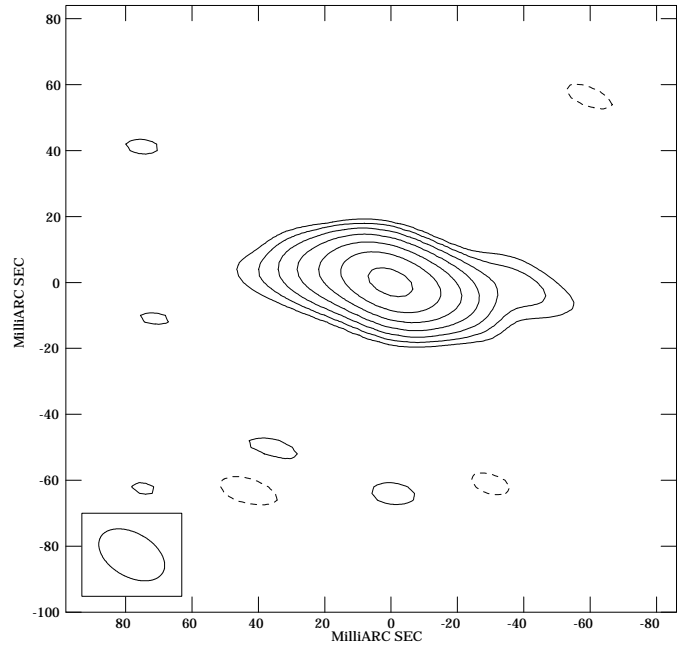


Fig. 1. Continuum image of NGC 4261 at 21 cm obtained with the EVN. The beam size is 21×15 mas. The contours are plotted at levels 1, 2, 4, 8, 16, 32 and 64 mJy/beam, with a map peak intensity of 79 mJy/beam. The Eastern counterjet side is only slightly weaker at this frequency.

tered on the reference position of the self-cal process; but is offset from the core. The sign of the phase on the Jodrell Bank – Westerbork baseline suggests that the absorption is preferentially on the Eastern (counterjet) side. Fig. 2 shows the absorbed flux density integrated at the supposed position of the main counterjet component located 18 mas to the East of the core (see below).

From the VLA spectrum presented in the Jaffe & McNamara (1994) paper, we estimate a total integrated absorbed flux density of 604 ± 168 mJy km/s, compared to the corresponding number for our VLBI spectrum; 409 ± 55 mJy km/s. The amount of VLBI scale absorption is therefore consistent with the VLA observations. Although we cannot exclude the possibility of additional H I absorbing gas on scales larger than sampled by the VLBI observations, we feel confident that we detect the bulk of the absorbing gas.

In making quantitative estimates of the opacity toward different source components we applied a model-fitting technique based on the three component model used to fit the continuum data. We first averaged the Jodrell – Westerbork spectral absorption data in frequency over the line width and then fitted the resulting phase and amplitude versus time using a three component Gaussian model based on the continuum model. Each Gaussian had the same fixed shape and position as that fitted to the continuum data, only the amplitude of each component was allowed to vary. The minimised χ^2 is achieved when most of the absorption is on the counterjet, a possible small absorption at the core and no absorption against the jet component. Fixing the jet absorption at zero we obtained the χ^2 -landscape shown in Fig. 3 for different combinations of counterjet and core absorp-

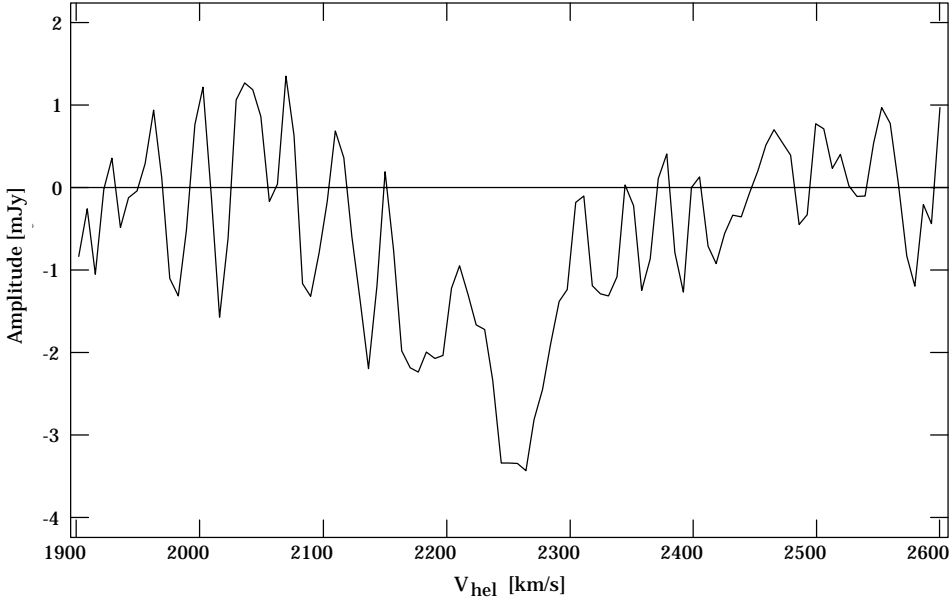


Fig. 2. Absorbed flux density for the Jodrell Bank – Westerbork baseline integrated 18 mas to the East of the map centre, i.e. at the counterjet side. The continuum has been subtracted. One spectral channel corresponds to 27 km/s.

tion. From this we estimate the absorbed counterjet and core flux densities averaged over the line to be 1.5 ± 0.3 mJy and 0.7 ± 0.4 mJy respectively.

Dividing by the continuum flux densities of each component from the absorbed fluxes we can estimate line-averaged opacities of 0.11 ± 0.02 and 0.01 ± 0.01 against the counterjet and core respectively. It therefore appears that virtually all of the absorbing gas is against the counterjet. Integrating the opacity over the line we estimate a total H I column density towards the counterjet of $N_{\text{HI}} = 2.5 \times 10^{19} T_{\text{sp}} \text{ cm}^{-2}$ and $N_{\text{HI}} < 2.2 \times 10^{18} T_{\text{sp}} \text{ cm}^{-2}$ towards the core.

4. Discussion

Having most of the H I column located in front of the counterjet at a projected distance of ~ 2.5 pc is consistent with a number of previous results on NGC 4261. First, at distances closer to the nucleus we do not expect H I absorption, since we know the circumnuclear material is mostly ionised. This is shown by the free-free absorption at a projected radius of 0.2 pc inferred by Jones & Wehrle (1997). Secondly, NGC 4261 harbours an X-ray source ($\sim 10^{41}$ erg/s in the 0.2–1.9 keV range, Worrall & Birkinshaw 1994), which puts a limit on the total column density on the line of sight to the nucleus. The model presented by Worrall & Birkinshaw (1994) yields an upper limit on the total column density of $4 \times 10^{20} \text{ cm}^{-2}$. Given that the X-rays preferentially originate in the nucleus, this fits in comfortably with the constraints from our VLBI H I absorption.

The model fitting from which we derive the optical depth does not allow the positions of the components to vary (see Sect. 3), nor is there any sensitivity for H I beyond the end of the continuum counter-jet. We are therefore forced to make a simplifying assumption, namely that 18 mas is the mean radius of the H I absorbing structure. This is supported by the fact that most of the VLA absorption is recovered by the VLBI observations (Sect. 3). Given the HST dust disk inclination, this

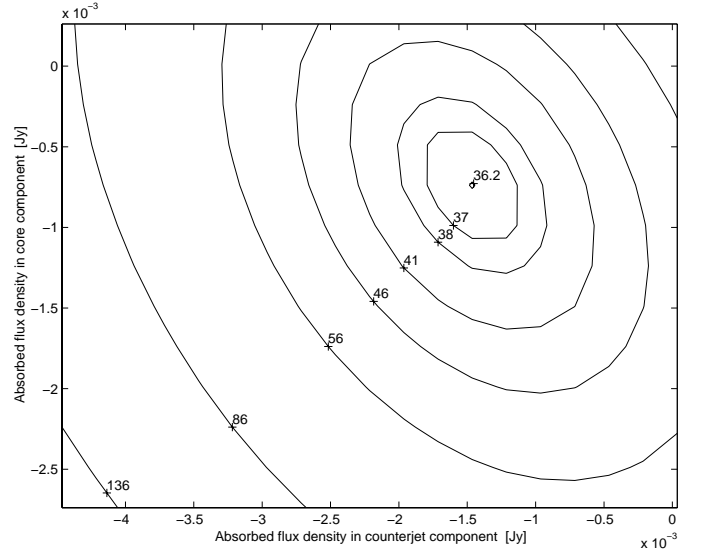


Fig. 3. The χ^2 -landscape achieved when varying the amount of absorbed flux over the counterjet and the core. The best fitting point has $\chi^2 = 36.2$. Number of degrees of freedom=35.

implies a distance 5.7 pc away from the nucleus. The FWHM of the line is comparable with other H I absorption observations of circumnuclear gas (e.g. in Cyg A, Conway & Blanco 1995). Therefore, in the next step we assume that the atomic gas is part of such a circumnuclear rotating structure and not due to individual clouds randomly distributed in front of the continuum source. Such a model of the H I disk is supported by the nuclear parameters derived by Ferrarese et al. (1996) from HST data on optical transitions. They found a central mass of $4.9 \times 10^8 M_{\odot}$, which implies a rotational velocity of 610 km/s at the location of the H I. Under the standard assumption that the linewidth ΔV provides an estimate of the isotropic turbulent velocity, we use the thin disk relation $h \sim r(\Delta V/V_{\text{circ}})$ to estimate the disk

thickness h . We estimate the velocity dispersion ΔV at radius r to be ~ 130 km/s which gives $h = 1.3$ pc. So the H I is likely to reside in a thin circumnuclear disk with an opening angle of $\sim 13^\circ$. The average density can, assuming a volume filling factor f of unity, be estimated to be $n_{\text{HI}} = 6 \times 10^2 \text{ cm}^{-3}$ for a spin temperature of 100 K. It follows that a more clumpy distribution ($f < 1$) will increase the estimated density ($\propto f^{-1/3}$) and decrease the estimated mass ($\propto f^{2/3}$). However, adopting $f = 1$ for simplicity, a mass estimate of H I inside an homogeneous disk of radius 6 pc is $M_{\text{HI}} \sim 2 \times 10^3 M_\odot$. Such a mass would be enough to supply material to the source for $< 3 \times 10^7$ years (assuming a radiative efficiency $\eta < 10\%$), given that the total luminosity of the radio source is $\sim 3.6 \times 10^{41}$ erg/s (e.g. Ferrarese et al. 1996). Using the correlation between FRI source sizes and their age (Parma et al. 1999), the size of NGC 4261 (Jaffe & McNamara 1994) implies an age $\sim 3 \times 10^7$ years. The same correlation shows other FRIs with ages $> 10^8$ years. Hence, on this time-scale the H I mass we estimate is barely sufficient to fuel the source. It seems more plausible that there is a continuous flow of accreting material being transported from the 100 pc scale dust disk onto the central nucleus.

The circumnuclear torus- or disk-structures observed in H I are usually found on slightly larger scales (50 – 100 pc; e.g. Gallimore et al. 1999 and Conway 1999). Only in a few other cases the H I is found to lie on very small scales (< 10 pc in NGC 4151; Mundell et al. 1996 and Gallimore et al. 1999) and it is not obvious that H I survives so close to the nucleus. For gas irradiated by X-rays an effective ionisation parameter ξ_{eff} can be defined, which governs the physical state of the gas (Maloney et al. 1996). For $\xi_{\text{eff}} < 10^{-3}$ the gas is likely to be molecular with gas temperatures close to or below 100 K, while higher values of ξ_{eff} correspond to a hotter atomic gas phase. Following Maloney et al. (1996), we use $\xi_{\text{eff}} = L_x / (r^2 n N_{22}^{0.9})$, where L_x is the hard (> 1 keV) X-ray luminosity, r is the distance from the nucleus to the irradiated gas, n is the gas density and N_{22} is the column density in units of 10^{22} cm^{-2} . At the distance of 6 pc a gas density of $6 \times 10^2 \text{ cm}^{-3}$ yields an (atomic) obscuring column density of $N_{22} \sim 1.1$. Using the hard X-ray luminosity of NGC 4261 (10^{41} erg/s, Roberts et al. 1991) this results in $\xi_{\text{eff}} = 0.5$; thus implying a mainly atomic gas phase where the gas temperature is likely to exceed 1000 K (Maloney et al. 1996). As a consequence the spin temperature is probably larger than 100 K, and our estimates of the H I mass and density will only be lower limits.

We conclude that within the scope of this model, it is indeed possible to have an atomic structure on the scales sampled by our VLBI observations. The inner boundary of this region is naturally set by the location of the free-free absorption, which also

must be geometrically thin in order to leave the core unattenuated. On the outside, the structure changes over into a dust disk which is visible to HST from its innermost pixel, at $r \sim 6$ out to 240 pc. However, since one would think that the mm radiation originates from the flat spectrum core, it is difficult to reconcile the reported CO absorption (Jaffe & McNamara 1994) with a thin molecular disk. Apart from the unknown location of the CO gas, the evidence points to the FRI radio-source in NGC 4261 being powered by gas infall through a relatively thin disk with a clear gradient of excitation conditions.

Acknowledgements. The scientific observations presented in this paper were made possible by the dedication and expertise of the teams involved in constructing the EVN MkIV data processor and implementing the EVN MkIV upgrade at the stations. We acknowledge especially the effort required by the correlator team to produce the data for this project in a such an early stage.

References

- Conway J.E., 1999, In: C.L. Carilli, S.J.E. Radford, K.M. Menten, & G.I. Langston (eds.) *Highly Redshifted Radio Lines*, ASP Conf. Series Vol. 156, p. 259
- Conway J.E. & Blanco P.R., 1995, *ApJ*, 449, L131
- Ferrarese L., Ford H.C. & Jaffe W., 1996, *ApJ*, 470, 444
- Ford H.C., Harms R.J., Tsvetanov Z.I., Hartig G.F., Dressell L.L., Kriss G.A., Bohlin R.C., Davidsen A.F., Margon B., Kochhar A.K., 1994, *ApJ*, 435, L27
- Gallimore J.F., Baum S.A., O’Dea C.P., Pedlar A. & Brinks E., 1999, *ApJ*, 524, 684
- Jaffe W., Ford H.C., Ferrarese L., van den Bosch F. & O’Connell R.W., 1993, *Nature*, 364, 213
- Jaffe W. & McNamara B.R., 1994, *ApJ*, 434, 110
- Jaffe W., Ford H.C., Ferrarese L., van den Bosch F. & O’Connell R.W., 1996, *ApJ*, 460, 214
- Jones D.L. & Wehrle A.E., 1997, *ApJ*, 484, 186
- Maloney P.R., Hollenbach D.J. & Tielens A.G.G.M., 1996, *ApJ*, 466, 561
- Mundell C.G., Pedlar A., Baum S.A., O’Dea C.P., Gallimore J.F. & Brinks E., 1996, *VA*, 40, 97
- Nolthenius R., 1993, *ApJS*, 96, 9
- Parma P., Murgia M., Morganti R., Capetti A., de Ruiter H.R. & Fanti R., 1999, *A&A*, 344, 7
- Tacconi L.J. Genzel R., Blietz M., Cameron M., Harris A.I. & Madden S., 1994, *ApJ*, 426, L77.
- Taylor G.B. 1996, *ApJ*, 470, 394
- Roberts M.S, Hogg D.E., Bregman J.N., Forman W.R. & Jones C., 1991, *ApJS*, 75, 751
- Rydbeck G., Wiklind T., Cameron M., Wild W., Eckart A., Genzel R. & Rothermel H., 1993, *A&A*, 270, L13.
- Worrall D. & Birkinshaw M., 1994, *ApJ*, 427, 134